



Synthesis and Characterization of Biobased Isosorbide-Containing Copolyesters as Shape Memory Polymers for Biomedical Applications

Journal:	<i>Journal of Materials Chemistry B</i>
Manuscript ID:	TB-ART-08-2014-001304.R1
Article Type:	Paper
Date Submitted by the Author:	12-Sep-2014
Complete List of Authors:	Kang, Hailan; Beijing University of Chemical Technology, Li, Manqiang; Beijing University of Chemical Technology, Tang, Zhenghai; South China University of Technology, Xue, Jiajia; Beijing University of Chemical Technology, Hu, Xiaoran; Beijing University of Chemical Technology, Zhang, Liqun; Beijing University of Chemical Technology, Key Laboratory of Beijing City for Preparation and Processing of Novel Polymer Material; Beijing University of Chemical Technology, State Key Laboratory of Organic/Inorganic Composites Guo, Baochun; South China University of Technology,

ARTICLE

Synthesis and Characterization of Biobased Isosorbide-Containing Copolyesters as Shape Memory Polymers for Biomedical Applications

Cite this: DOI: 10.1039/x0xx00000x

Hailan Kang,^{a,d} Manqiang Li,^{a,b} Zhenghai Tang^c, Jiajia Xue,^{a,b} Xiaoran Hu,^{a,b} Liqun Zhang,^{*,a,b} Baochun Guo^{*,c}

DOI: 10.1039/x0xx00000x

www.rsc.org/

Novel biobased isosorbide-containing copolyesters (PBISI copolyesters) with both biocompatibility and sustainability were synthesized by using commercially available biobased diols and diacids. Due to the presence of itaconate in copolyester, it can be readily crosslinked by peroxide into a crystallizable network. The structure and thermal properties of PBISI copolyesters were determined by ¹H NMR, FTIR, DSC, and WAXD. The chain composition, melting point and crystallinity of the PBISI copolyesters can be tuned continuously by changing the content of isosorbide. The crosslinked copolyester is demonstrated to be a promising shape memory polymer (SMP) with excellent shape memory properties including shape fixity and shape recovery rate close to 100%. The switching temperatures of PBISI-based SMPs can be tuned between 26 °C and 54 °C by altering the composition of PBISI copolyesters and curing extent. Cell adhesion and proliferation were adopted to evaluate the potential biocompatibility of PBISI-based SMPs, and the results indicated that all the PBISI-based SMPs were essentially noncytotoxic, making them suitable for fabricating biomedical devices.

1 Introduction

Shape memory polymer (SMP) is a stimuli-responsive smart polymer that can fix a temporary deformed shape and recover its original permanent shape upon exposure to external stimuli, such as heat, light, electricity, and magnetism.¹⁻⁵ So far, the most extensively investigated SMPs have been thermo-responsive SMPs, which are triggered by heat. SMPs generally contain two networks: a permanent network, which determines the permanent shape and a temporary network, which fixes the temporary shape at temperatures below the switching temperature (T_{trans}). The permanent network can be obtained either by physical interaction or by chemical bonding, while the temporary network is typically formed by vitrification, crystallization, or some other physical interaction such as hydrogen bonding and ionic bonding.⁶⁻⁸ SMPs have numerous applications such as sensors, actuators, smart textiles, and self-deployable structures. Since SMPs can promote minimally invasive surgery and provide structural support, they have generated substantial interests in biomedical applications, such as drug delivery, biosensors and biomedical devices, and implant materials.⁹⁻¹¹ Xue et al.¹⁰ synthesized novel SMPs containing three-armed poly(ϵ -

caprolactone) as the switching segment and poly[(R)-3-hydroxybutyrate-co-(R)-3-hydroxyvalerate] as the hard segment for fast self-expandable stents. Nagahama et al.¹² prepared biodegradable SMPs as a controlled drug release device by crosslinking star shape branched oligo(ϵ -caprolactone) with hexamethylene diisocyanate. However, the reported SMPs in biomedical devices were mostly based on petroleum-dependent polymers.

Synthesis of biobased polymers from renewable resources instead of petroleum-based raw materials is indeed a feasible solution to the growing environmental threat and the depletion in fossil feedstocks.¹³⁻²² Although biobased SMPs have been reported, SMPs derived from the industrially produced monomers, especially those in large quantities, are still few. Consequently, the design and synthesis of biobased SMPs are important and highly desired. Carbohydrate-based derivatives have been extensively explored as suitable monomers for the synthesis of biobased polymers because carbohydrates are the most abundant biomass feedstock. Among carbohydrate-based monomers, those with a cyclic structure, such as isosorbide²⁰ or 2,5-furandicarboxylic acid²³, stand out for providing polycondensates with improved properties, especially those related

to polymer chain stiffness. Isosorbide (1,4:3,6-dianhydro-D-glucitol, ISB), a biomass monomer derived from glucose, is the only bicyclic carbohydrate-based monomer commercially available at an industrial level. Because of its rigid molecular structure and chirality, ISB has been extensively used in synthesizing polyesters²⁴⁻²⁶, polyurethanes²⁷, polyamides²⁸ and polycarbonates²⁹. Noordover et al.²⁵ prepared aliphatic polyesters with high T_g for powder coatings by introducing ISB units into polyesters. Polyterephthalates containing a small fraction of ISB, such as poly(ethylene terephthalate)³⁰ and poly(butylene terephthalate)³¹, can broaden the industrial applications of polyesters, such as packaging (bottles, films) and molded parts. However, there is still no attempt to prepare biobased SMPs by the copolycondensation of isosorbide with others biobased monomers.

The expected biocompatibility and biodegradability based on structural characteristics of biobased polymers make these materials potentially promising for biomedical applications, especially in the area of minimally invasive surgery. For example, a bulky medical device can be inserted into the body in a compressed temporary shape through a small surgical incision. The implant returns to its application permanent shape when the temperature is raised to above T_{trans} . After a defined time the device degrades, thus eliminating a second surgery for its removal.⁶ For such applications, thermo-responsive SMPs should exhibit highly temperature-sensitive shape recovery at switching temperatures slightly above normal human body temperature (37 °C). Meanwhile, the delicate tenability of switching temperature is also important in the biomedical applications of SMPs as different switching temperatures are needed for different requirements.

In this study, we designed and synthesized novel biobased poly(butanediol/isosorbide/sebacate/itaconate) copolyesters (PBISI copolyesters) containing isosorbide as thermally induced SMPs. The SMP performance can be easily tuned by adjusting the structure of the copolyester chains. In our design, four biobased monomer reactants isosorbide, butanediol, itaconic acid, and sebacic acid, which are industrially available in large quantities, were utilized for the polycondensation. The pendent double bonds were introduced into the chains by itaconic acid, which were subsequently crosslinked into the permanent network. ISB was introduced to adjust the chain flexibility and the T_{trans} . The effects of ISB content and the extent of cure on the properties of PBISI-based SMPs, such as microstructures, thermal properties, mechanical properties, and shape-memory behavior, were investigated. The cell adhesion and proliferation on the PBISI substrates were performed to evaluate their potential biocompatibility of the substrates.

2 Experimental

2.1 Raw Materials

Itaconic acid (IA) (purity 99.0%), sebacic acid (SA) (purity 99.0%), 1,4-butanediol (BDO) (purity 99.0%), 1,4:3,6-dianhydro-D-glucitol (isosorbide, ISB) (purity 99.0%), and tetrabutyl titanate (TBT) were purchased from Alfa Aesar. Tri-(4-hydroxy-tetramethyl-piperidin-1-oxyl) phosphite (4-hydroxy-TEMPO) phosphite was supplied by Beijing Additive Institute. Chloroform and methanol were provided by Beijing

Yili Fine Chemical Co., Ltd. The dicumyl peroxide (DCP) used was a commercial product.

2.2 Synthesis of Poly(butanediol/isosorbide/sebacate/itaconate) (PBISI) Copolyesters

The PBISI copolyesters were synthesized by a typical polycondensation reaction. The molar ratios diols/diacids and SA/IA are fixed at 1.1:1 and 0.85:0.15, respectively. The content of ISB relative to the total amount of diols varied from 0 mol% to 40 mol%. A 10% molar excess of diol to diacid, tri-(4-hydroxy-TEMPO) phosphite as the antioxidant (0.05 wt% relative to the total reactants), and tetrabutyl titanate (TBT) as the catalyst (0.05 wt% relative to the total reactants) were used. Using a slight excess of diol in the polycondensation is a common practice for the synthesis of polyesters both in the laboratory and in industry. The excess diols were removed under the high temperature and low vacuum at the last stage of the polycondensation reaction. An exemplary polymerization of ISB, BDO, IA, and SA was accomplished as follows: ISB (8.03 g, 0.055 mol), BDO (19.8 g, 0.22 mol), IA (4.875 g, 0.0375 mol), and SA (42.925 g, 0.2125 mol) were introduced into a 100-ml three-necked flask equipped with a mechanical stirrer, a nitrogen inlet, and a vacuum distillation outlet. The reaction mixture was heated to 180 °C and allowed to react for 2 h under a low nitrogen flow, and then the catalyst TBT was added to the reaction system. The mixture was further heated to 220 °C under reduced pressure (<300 Pa) for 4–10 h until the “Weissenberg effect” was observed. The resulting copolyesters were dissolved in chloroform and precipitated in excess of cold methanol to remove the unreacted monomers and the formed oligomers. Finally, the copolyesters were collected by filtration, washed repeatedly with methanol, and dried under vacuum. The copolyester containing 20 mol% of isosorbide relative to the amount of total diols was denoted as PBISI-2 copolyester. For comparison purposes, PBSI copolyester was synthesized from BDO, SA, and IA, and PISI copolyester was synthesized from ISB, SA, and IA.

2.3 Preparation of Crosslinked PBISI Copolyesters

For the preparation of PBISI-based SMPs, the PBISI copolyesters were mixed with DCP in chloroform. The mixture was dried under vacuum and compression molded at 160 °C for 20 min.

2.4 Measurements

Molecular weights were measured by gel permeation chromatography (GPC) on a Waters Breeze instrument equipped with three water columns (Stearge HT3_HT5_HT6E) by using tetrahydrofuran as the eluent (1 ml/min) and a Waters 2410 refractive index detector. A polystyrene standard was used for calibration. Proton nuclear magnetic resonance (¹H NMR) spectra of PBISI copolyesters with deuterated chloroform (CDCl₃) as the solvent were recorded on a Bruker AV400 spectrometer at room temperature. Fourier transform infrared (FTIR) spectra were obtained on a Bruker Tensor 27 spectrometer. The measurement resolution was set at 4 cm⁻¹,

and the spectra were collected in the wavenumber range of 600 to 4000 cm^{-1} . Thermal stability was evaluated by thermogravimetric analysis (TGA, Mettler-Toledo International Inc., Switzerland). Samples of 10 mg were heated from 40 °C to 700 °C at a heating rate of 10 °C/min under nitrogen. Differential scanning calorimetry (DSC) measurements were performed with a Mettler-Toledo DSC instrument under nitrogen atmosphere at a heating rate of 10 °C/min from -80 °C to 120 °C and a cooling rate of 10 °C/min from 120 °C to -80 °C. Wide-angle X-ray diffraction (WAXD) studies were conducted on a Rigaku RINT diffractometer with Cu K radiation (40 kV, 200 mA) in the 2θ range of 5° to 50° at a scan rate of 5°/min.

Tensile tests were performed with dumbbell-shaped samples according to ASTM D412 by using a CMT 4104 electrical tensile instrument (Shenzhen SANS Test Machine Co. Ltd., China) at a crosshead speed of 50 mm/min and 23 °C. The tensile tests at elevated temperature were performed by using a Q800 dynamic mechanical analyzer (TA, USA). After being equilibrated at melting temperature (T_m) +10 °C for 10 min, the tensile test was initiated at 0.05 N/min and allowed to continue until fracture. At least five samples were tested to obtain an average value.

The thermomechanical cycles were generated with the Q800 dynamic mechanical analyzer to characterize the shape memory behavior of PBISI-based SMPs. Prior to deformation, the samples were heated to 20 °C above T_m and equilibrated for 10 min. In step 1 (deformation), the sample was deformed by ramping force from a preload of 0.005 N to a designed strain (ϵ_m) at a rate of 0.05 N/min. In step 2 (cooling), the sample was cooled to 30 °C below T_m at a rate of 3 °C/min to fix the deformation. In step 3 (unloading and shape fixing), the force on the sample was unloaded to the preload value (0.005 N) at a rate of 0.05 N/min, and then kept at a constant temperature of 30°C below T_m for 10 min to ensure shape fixing. Upon unloading, part of the strain ($\epsilon_m - \epsilon_u$) was instantaneously recovered, leaving an unloading strain (ϵ_u). In the final step (recovery), the sample was reheated at a rate of 3 °C/min to 20 °C above T_m and held there for 10 min to recover any residual strain. The recovery process left a permanent strain ($\epsilon_{p(N)}$). This thermomechanical cycle was repeated three times on the same sample. The shape fixity (SF) and shape recovery (SR) were defined as

$$SF(\%) = \frac{\epsilon_u}{\epsilon_m} \times 100 \quad (1)$$

$$SR(\%) = \frac{\epsilon_m - \epsilon_{p(N)}}{\epsilon_m - \epsilon_{p(N-1)}} \times 100 \quad (2)$$

Cell adhesion and proliferation were evaluated by Cell Counting Kit-8 (CCK-8) assay. Round specimens of 20 mm diameter were sterilized and then fixed on a 24-well plate (Sigma, USA). L929 mouse fibroblast cells were used and cultured in Dulbecco's modified Eagle's medium (DMEM) with 10% fetal bovine serum (FBS) and antibiotics (100 $\mu\text{g}/\text{mL}$ penicillin and 100 mg/mL streptomycin) at a density of 4.0×10^4 cells/mL. Then 800 μL of cell culture medium and 100 μL of

cell suspension were added into the wells, while the cell suspension was added into one well with no specimen to be used as a control. The cells were incubated in 5% CO_2 atmosphere at 37 °C. After being incubated for 4 h, each specimen was washed with PBS three times to remove the cells that did not adhere to the specimen and 100 μL of WST-8 (final dilution: 1:10) was added onto the specimen to test the live cells. After being incubated for 1 and 3 days, 100 μL of supernatant was transferred into a 96-well plate and the plate was incubated for 3 h in the incubator. The absorbance at 450 nm was measured by using a microplate reader. For SEM observations, the cell-cultured specimens were washed three times with PBS, fixed with 3% glutaraldehyde at 4 °C for 2 h, and soaked in sucrose solution (0.18 mol/L) at 4 °C for 2 h. The specimens were then dehydrated by a series of graded ethanol solutions and finally lyophilized.

3. Results and discussion

3.1 Synthesis and Characterization of PBISI Copolyesters

The biobased copolyesters containing ISB were obtained by a two-step melt polycondensation reaction, as indicated in Scheme 1. The reaction was conducted in the melt to imitate the condition usually applied in industrial production. Copolyesters with ISB contents of 0 mol% to 100 mol% were prepared by using the familiar TBT catalyst and a small excess of diol with regard to diacid to compensate for the loss of volatiles. The polycondensation time increased gradually with the ISB content, confirming that ISB exhibits low reactivity of polycondensation. At ISB contents higher than 40 mol%, the “Weissenberg effect” cannot be observed, and the number-average molecule weight is lower than 10000 g/mol, as shown in Table 1. Extending the reaction time does not lead to further reaction because of the low reactivity of ISB, but increases side reactions. The GPC results of PBISI copolyesters with ISB contents of 0 mol% to 40 mol% are summarized in Table 1. The number-average molecular weights and polydispersity index (PDI) of the PBISI copolyesters vary between 15000 g/mol and 39000 g/mol and between 3.2 and 6.0, respectively. The molecular weights of PBISI copolyesters significantly decrease with increasing ISB content, a trend commonly observed in the synthesis of copolyesters containing cyclic diol comonomers, such as 2,3,4,5-di-*O*-methylene-galactitol and 2,4:3,5-di-*O*-methylene-*D*-glucitol,^{32,33} because of the increased difficulty of end chains with reduced mobility to meet one another.

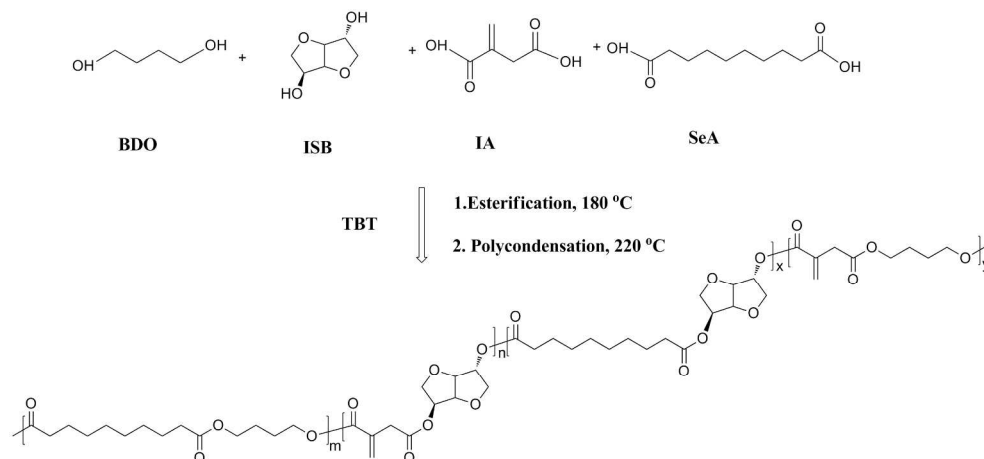
Table 1 Compositions and molecular weights of PBISI copolyesters

Samples	Molar compositions ISB/BDO		Molecular weights		
	Feed ^a	Copolyester ^b	M_n^c	M_w^c	PDI^d
PBISI	0:1	0:1	38845	125331	3.2
PBISI-1	0.1:0.9	0.08:0.92	31035	133450	4.3
PBISI-2	0.2:0.8	0.15:0.85	28716	145820	5.0
PBISI-3	0.3:0.7	0.22:0.78	20923	110887	5.3
PBISI-4	0.4:0.6	0.28:0.72	15093	90678	6.0
PBISI-6	0.6:0.4	0.46:0.54	6455	22105	3.4
PISI	1:0	1:0	4835	10917	2.2

^a Molar ratio in the initial feed.

^b Molar ratio in the copolyester determined by ¹H NMR.

^c Number- and weight-average molecular weights (M_n and M_w) and polydispersity index (PDI) determined by GPC.



Scheme 1. Polymerization reactions leading to PBISI copolyesters.

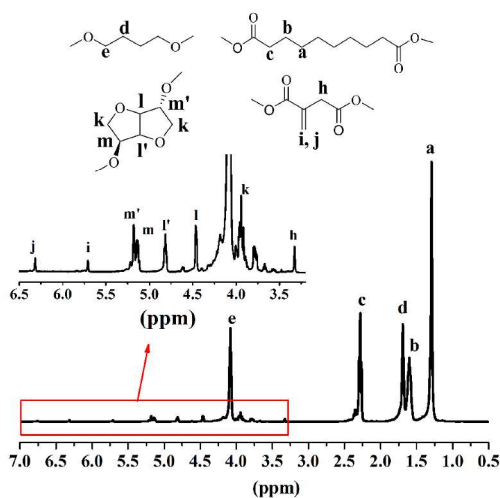


Fig. 1 ^1H NMR spectrum of PBISI-2 copolyester.

The chemical structures and compositions of the PBISI copolyesters were evaluated by using ^1H NMR spectroscopy. An example illustrating this evaluation is provided in Fig. 1, which shows the spectrum of PBISI-2 copolyester with the assignments for all proton signals. The peaks at δ 1.29, δ 1.60, and δ 2.28 ppm are from the protons of the methylene groups in sebacic acid, $-(\text{CH}_2)_4-\text{CH}_2-\text{CH}_2-\text{COO}-$. The peaks at δ 1.69 and δ 4.08 ppm originate from the protons of butanediol, $-(\text{CH}_2)_2-\text{CH}_2-\text{O}-$. The chemical shifts at δ 6.31, δ 5.71, and δ 3.33 ppm corresponds to $-\text{CO}-\text{C}(\text{=CH}_2)-\text{CH}_2-$, demonstrating the introduction of pendent alkene groups to the PBISI macromolecular chains. The peaks at δ 3.94, δ 4.47, δ 4.81, δ 5.14, and δ 5.18 ppm are assigned to the protons of ISB. Additionally, the molar ratio of ISB to BDO was calculated from the relative peak areas of the protons of each diol in the ^1H NMR spectra, and the results are given in Table 1. The content of ISB in each PBISI copolyester is obviously lower than that in the corresponding feed, more than 30% lower in some cases (Table 1). Similar losses of ISB were reported in the copolymerization of

mixtures of ISB and BDO with dimethyl terephthalate.²⁴ Such losses are attributed to the lower reactivity of the secondary hydroxyl groups of ISB than that of the primary hydroxyl groups of BDO.

All the bio-based PBISI copolyesters were additionally analyzed by FTIR spectroscopy. In Fig. 2, all the FTIR spectra are very similar. The peak for the hydroxyl group ($-\text{OH}$) stretching vibration at 3000 cm^{-1} to 4000 cm^{-1} has not been found, indicating complete reaction of the monomers. The PBISI copolyesters show typical carbonyl stretching vibration peaks at 1732 cm^{-1} and 1171 cm^{-1} , indicating the formation of ester bonds. The peaks at 1646 cm^{-1} and 803 cm^{-1} are assigned to the stretching vibrations and the rocking vibration of carbon-carbon double bonds ($\text{C}=\text{C}$), respectively. The peaks at both 2930 cm^{-1} and 2856 cm^{-1} are assigned to the methylene ($-\text{CH}_2-$) stretching vibration. A comparison of the FTIR spectra of PBSI and PBISI copolyesters shows that a new absorption at 1094 cm^{-1} is observed for PBISI copolyesters, corresponding to the $\text{C}-\text{O}-\text{C}$ stretching vibration of the ether bonds of ISB. The intensity of this new peak significantly increases with increasing content of ISB.

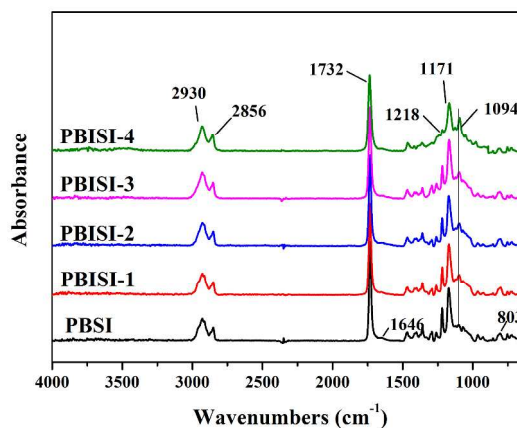


Fig. 2 FTIR spectra of PBISI copolyesters.

Table 2 Thermal and crystallization properties of PBISI copolyesters.

Samples	TGA			DSC					Crystallinity ^f (%)
	T_d^a (°C)	T_d^b (°C)	RW ^c (%)	Second heating ^e			Cooling ^e		
				T_g^d (°C)	T_m (°C)	ΔH_m (J/g)	T_c (°C)	ΔH_c (J/g)	
PBSI	318	413	6%	-51.2	59.8	80.1	40.8	74.7	61.3
PBISI-1	321	415	5%	-49.8	56.7	72.5	38.3	69.6	60.2
PBISI-2	338	418	4%	-44.7	52.9	59.5	30.0	57.1	53.7
PBISI-3	352	421	7%	-39.9	45.5	53.5	24.1	52.9	41.2
PBISI-4	370	424	10%	-34.8	33.7	40.7	4.8	40.5	32.6

^a Temperature at which a 5% weight loss was observed in the TGA traces recorded at 10 °C/min.

^b Temperature of maximum degradation rate.

^c Remaining weight after heating at 600°C.

^d Glass-transition temperature (T_g) taken as the inflection point of a second heating DSC trace recorded at 10 °C min⁻¹.

^e Melting (T_m) and crystallization (T_c) temperatures and their respective enthalpies (ΔH_m , ΔH_c) measured by DSC at heating/cooling rates of 10 °C min⁻¹.

^f Calculated from WAXD results.

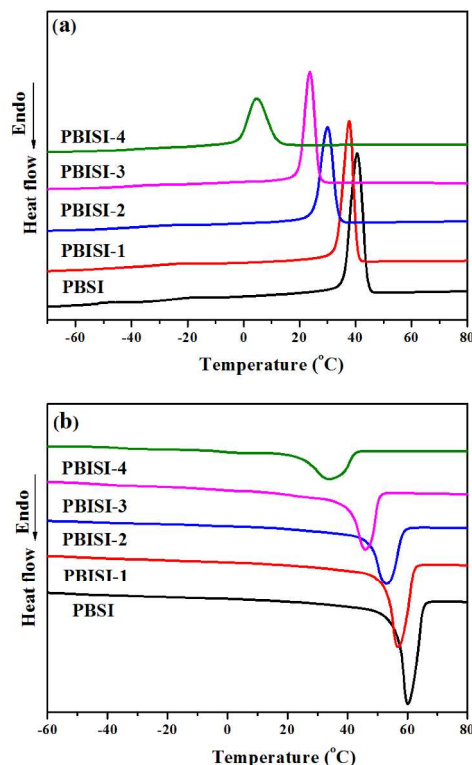
3.2 Thermal Properties of PBISI Copolyesters

Thermogravimetric analysis was conducted in an inert atmosphere by TGA and the results are shown in Fig. S1 and Table 2. The thermal decomposition of PBISI copolyesters take place in one stage, with the maximum rate occurring at 300–450°C, leaving a final weight less than 10% of the initial weight at 600 °C. The onset decomposition temperature at 5% of weight loss ($T_{d, 5\%}$) and the maximum decomposition temperature ($T_{d, max}$) steadily increase with increasing ISB content, corroborating that the introduction of ISB enhances the thermal stability of these copolyesters. Overall, all PBISI copolyesters display a satisfactory thermal stability with an onset decomposition temperature higher than 340 °C, meeting the requirement of most applications.

The bicyclic ISB structure is stiff, bulky and asymmetric, which would reduce the regularity and flexibility of the polymer chains. Thus, the incorporation of ISB in the polymer chains significantly alters the thermal transitions of PBISI copolyesters. The DSC traces of the PBISI copolyesters are depicted in Fig. 3, and the thermal data are summarized in Table 2. The glass transition temperatures (T_g) of the copolyesters could be detected in the heating DSC tracing of samples cooling from the melt. The T_g increases with the content of ISB units because the ISB structure confers stiffness to the polymer chain and therefore reduces the free volume. The PBISI copolyesters exhibit sharp and intense crystallization peaks during cooling. The crystallinity of PBISI copolyesters decreases rapidly with increasing content of ISB units. All samples display endothermic peaks characteristic of melting at temperatures decreasing from 60 °C to 34 °C and with intensity decreasing with increasing ISB content. The introduction of ISB units into PBISI copolyesters not only increases the sequence randomness of the macromolecular chains but also restricts the segmental mobility, resulting in the decrease in T_c , T_m , the enthalpy of crystallization (ΔH_c), and the enthalpy of melting (ΔH_m), but the increase in T_g . The DSC results clearly show that the T_m of PBISI copolyesters can be tuned by adjusting the ISB/BDO ratio.

The X-ray diffraction results of copolyesters are consistent with the DSC results. The WAXD patterns of PBSI copolyester and PBISI copolyesters are depicted in Fig. 4. The presence of sharp reflection peaks corroborated the semicrystalline nature of the

copolyesters. All the samples show similar diffraction peaks around 21.5° and 24.6°, and the intensity of the diffraction peaks decreases with the content of ISB. These results indicate that the SA-BDO sequences are crystalline, whereas the SA-ISB sequences remain amorphous. By deconvolution of the diffraction patterns, the crystallinity of the semicrystalline PBISI copolyesters can be calculated. As shown in Table 1, the crystallinity of PBISI copolyesters gradually decreases with the increase of ISB content. Such a delay in crystallization may be due to a diminished chain mobility and/or difficulty in chain packing, similar to that in other copolymers containing ISB, as reported in the literatures.^{24, 30}

**Fig. 3** DSC traces of PBISI copolyesters (a) cooling; (b) second heating.

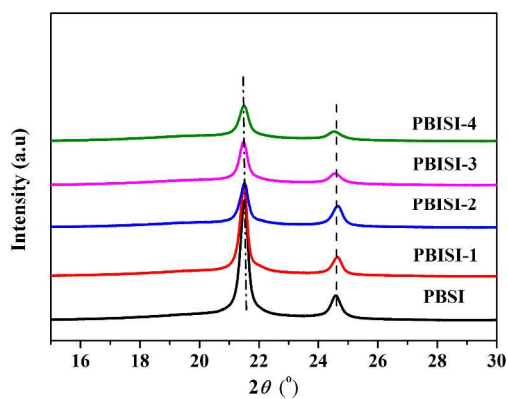


Fig. 4 WAXD patterns of PBISI copolyesters.

3.3 Shape Memory Switching Temperature of PBISI-based SMPs

A critical parameter for SMP is its shape memory switching temperature (T_{trans}). A SMP can memorize its temporary shape below T_{trans} and subsequently recover its permanent shape upon heating above T_{trans} . A PBISI-based SMP, which is a semicrystalline copolyester, can fix the deformed shape by the crystalline part and the chain entanglements of the PBISI copolyester. Therefore, the deformation and shape recovery of PBISI copolyester can be attributed to the melting and crystallization of the crystalline segments of the copolymer. So the T_{trans} of PBISI-based SMPs is determined by the T_m . ISB was employed to modify the chain sequence of the copolyesters and so as to alter the T_m , and the change in T_m in turn changes the T_{trans} . Alternatively, the crosslinking of PBISI copolyesters restrains the crystallization and decreases the T_m . The T_m of PBISI-based SMPs as a function of ISB molar fraction and DCP content is shown in Fig. 5. As shown by the DSC results, the T_m of PBISI-based SMPs decreases with the increase in ISB content and the curing extent. The crosslinking of PBISI copolyesters suppresses the chain mobility and increases the sequence randomness, thus reducing the size of the crystallite and lowering the T_m . Fig. 5 clearly shows that T_m of PBISI-based SMPs can be finely tuned, in the range of 26 °C to 54 °C, by changing the composition and the curing extent of the PBISI copolyesters. For biomedical applications, the T_{trans} values of PBISI-based SMPs can potentially be adjusted around or above the body temperature (37 °C) by tuning the ISB content and the curing extent.

Table 3 Thermal and crystallization properties of PBISI-2 copolyester with different DCP content

DCP (phr)	T_g (°C)	T_m (°C)	ΔH_m (J/g)	T_c (°C)	ΔH_c (J/g)	Crystallinity ^a (%)
0	-44.7	52.9	59.5	30.0	57.1	53.7
0.2	-43.8	49.6	57.1	22.2	54.0	50.5
0.4	-43.1	45.9	54.4	19.8	53.7	44.1
0.6	-42.7	45.3	50.5	18.0	49.7	40.2
0.8	-42.5	45.1	49.2	17.9	49.1	39.9

^a Calculated from WAXD method.

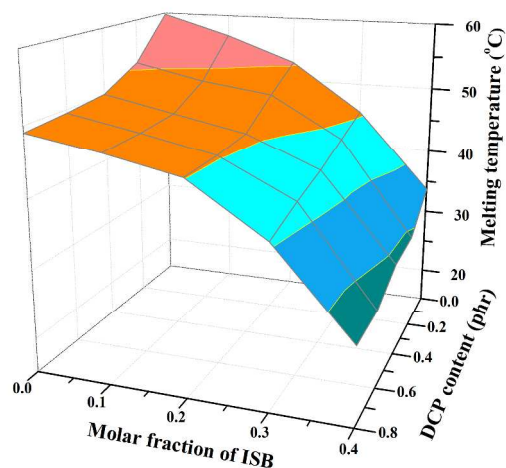


Fig. 5 T_m of PBISI-based SMPs as a function of ISB molar fraction and the curing extent.

The DSC traces (Fig. S2) and WAXD patterns (Fig. S3) for PBISI-2 copolyester with different DCP contents were used to evaluate the possible effect of curing extent on T_{trans} , and the relevant data are summarized in Table 3. The T_m , T_c , ΔH_m , and ΔH_c of PBISI-2 copolyester decrease with increasing DCP content. These results indicate that the crosslinking restricts the chain mobility and constrains crystal growth. Specifically, the local chain mobility necessary for the insertion of chains into a growing crystal is suppressed in the neighborhood of a crosslink site.³⁴ This hypothesis is supported by the reduction in crystallinity with increasing DCP content, as calculated from the WAXD patterns (Table 3). Other researchers also observed the crystallization depression by crosslinking.^{13-15, 34}

3.4 Mechanical Properties of Crosslinked PBISI Copolyesters

The stress-strain curves of crosslinked PBISI copolyesters at room temperature are shown in Fig. 6(a), and the relevant data are summarized in Table S1. The crosslinked PBISI copolyesters behave like plastic and exhibit distinct yielding which is followed by stable neck growth. The tensile strength and elongation at break of the crosslinked PBISI copolyesters range from 6.1 to 16.4 MPa and 240% to 430%, respectively. The yield strength and tensile strength of crosslinked PBISI copolyesters decrease with the increase of ISB content because of the decreased crystallinity as indicated by the DSC and WAXD results. The stress-strain curves of the crosslinked PBISI copolyesters at $T_m+20^\circ\text{C}$ are shown in Fig. 6(b). All the samples behave like soft elastomers at the higher temperature, with much lower tensile strength and elongation at break than those at room temperature. The DCP content also affects the mechanical properties of the crosslinked PBISI copolyesters, and the results for PBISI-2 copolyester are shown in Fig. S4 and Table S2. With increasing DCP content, the tensile strength and elongation at break slightly decrease, since the increase in crosslink density further restricts the mobility of polymer chains and therefore restrains their crystallinity. The tensile strength and drawability of PBISI copolyesters are compatible with many natural tissues, such as human inferior cava vein (1.17 MPa)³⁵, ulnar cadaveric peripheral

nerve (0.5–0.6 MPa)³⁶, and porcine aortic heart valve (8.3 MPa)³⁷. The tensile results show that the mechanical properties of the crosslinked PBISI copolyesters are in wide ranges and more importantly, easily adjustable.

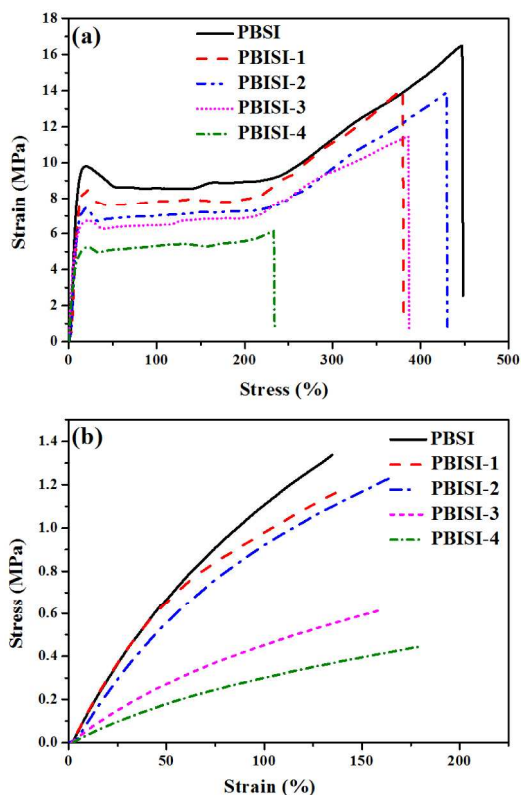
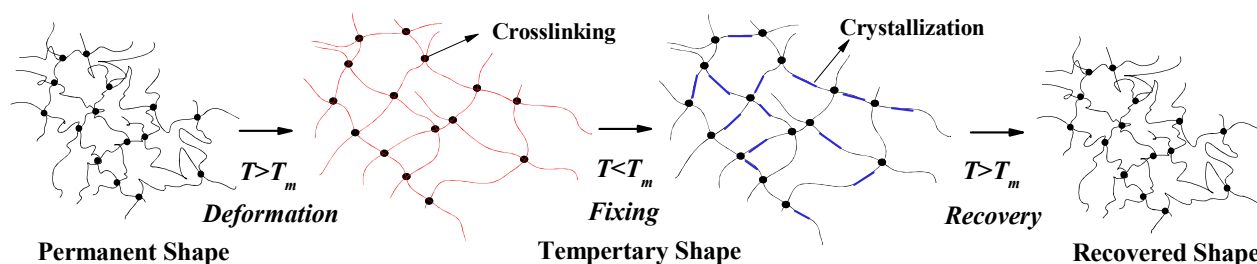


Fig. 6 Typical stress-strain curves of crosslinked PBISI copolyesters: (a) at room temperature; (b) at $T_m + 20^\circ\text{C}$. The samples were cured with 0.4 phr of DCP.

3.5 Shape Memory Behaviors of PBISI-based SMPs

The shape memory behavior of a PBISI-based SMP is triggered by switching the temperature below and above its T_m . As shown in Scheme 2, a PBISI-based SMP behaves as an elastomer above its T_m in permanent shape and can be deformed to a temporary shape under external force. If the deformed sample is cooled down to below its T_{trans} , the temporary shape is fixed. When the temperature is raised



Scheme 2 Molecular mechanism of PBISI-based SMP during shape recovery.

to above the T_{trans} again, the PBISI-based SMP would quickly return to its initial shape. For most practical applications, a quick recovery rate is desirable. The shape recovery rate of PBISI-2 SMP was measured by changing a film sample with a permanent linear shape into a temporary spiral shape at $T_m + 20^\circ\text{C}$, fixing this shape at $T_m - 30^\circ\text{C}$ for 10 min, and then placing the sample in a water bath at different temperatures. PBISI-2 SMP can completely recover to its initial shape within 16 s at temperature higher than 42°C . The shape recovery time of PBISI-2 SMP is depicted in Fig. 7. It can be seen that the curve based on the recovery time and temperature is converse S-shape. The shape recovery time is shorter when the PBISI-2 SMP is heated to higher temperatures. As the temperature exceeds 52°C , the shape recovery time reaches a constant value of about 4 s. The photographs illustrating the transformation of a PBISI-2 SMP film from a temporary spiral shape to the permanent linear shape are shown in Fig. 8.

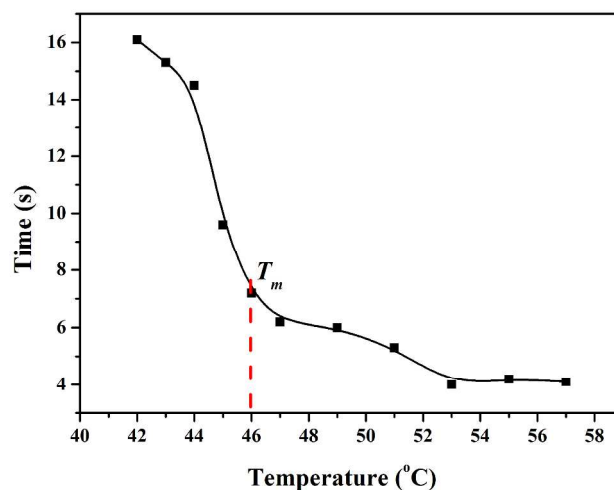


Fig. 7 Shape recovery time of PBISI-2 SMP as function of temperature. The sample was cured with 0.4 phr of DCP.



Fig. 8 Transition from the temporary spiral shape to the permanent linear shape for PBISI-2 SMP. The samples were cured with 0.4 phr of DCP and the recovery process was recorded after heating the samples to $T_m+10^\circ\text{C}$.

To further quantify the shape-memory behaviours, the cyclic thermomechanical tests of PBISI-based SMPs were performed to obtain the shape fixity rate (SF) and the shape recovery rate (SR). SF quantifies the ability of SMPs to fix the temporary shape in the cold state, while SR is a measure of the capacity of SMPs to recover the original shape. The stress-controlled programming cycles (three times) of PBISI SMP and PBISI-2 SMP are depicted in Fig. 9, and the two-dimensional recovery curves are also shown in Fig. S5. The cyclic curves appear reverse S-shaped during cooling, which is

induced by crystallization. For multiple cycling, the cyclic curves of all samples can overlap completely. All samples maintain excellent shape properties. The SF and SR values summarized in Fig. 10 shows that SF and SR increase slightly with increasing ISB content and cycle time. SF and SR are also independent of the cycle time. The SF and SR values of all samples are close to 100% after two cycles, indicating excellent shape memory properties.

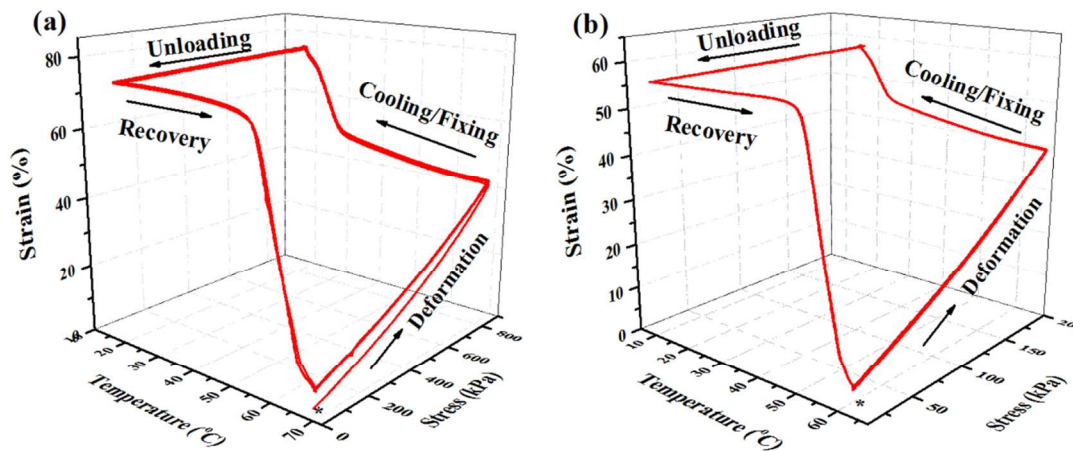


Fig. 9 Three-dimensional diagrams of stress-controlled programming cycles for (a) PBISI SMP and (b) PBISI-2 SMP. The samples were cured with 0.4 phr of DCP. An asterisk indicates the starting points for the cycling process.

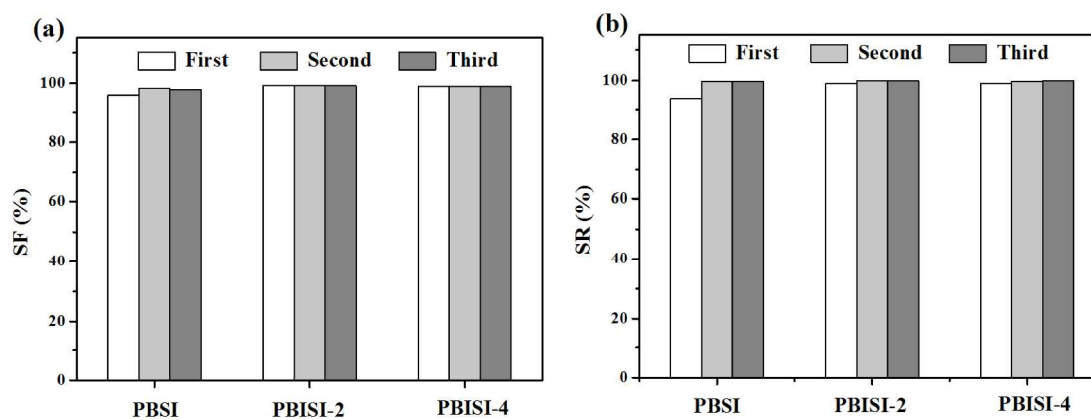


Fig. 10 SF and SR values of PBISI-based SMPs. The samples were cured with 0.4 phr of DCP.

3.6 Cell Adhesion and Proliferation of Crosslinked PBISI Copolyesters

The cytotoxicity of materials is evaluated to determine whether they are potentially suitable for biomedical applications in a specific environment. CCK-8 assay was adopted to evaluate the cytotoxicity of crosslinked PBISI copolyesters. Since the CCK-8 assay is specific to viable living cells and the non-adherent cells can be washed out, it reveals not only the cell adhesion and proliferation, but also the cytotoxicity of a material. In our cytotoxicity assays, the number and morphology of L929 mouse fibroblasts cells in the extract were observed. Fig. 11 shows the optical density (OD) (illustrating the viability) of L929 cells that were incubated for 1 and 3 days on the surface of various crosslinked PBISI copolyesters. The OD reflect the number of live cells indirectly. The OD continually increases with increasing culturing time. The crosslinked PBISI copolyesters show a slower growth rate of cells than polylactide (PLA), which is an acknowledged biocompatible polymer, because of the difference in biocompatibility between the two materials. However, the crosslinked PBISI copolyesters did not inhibit cell proliferation, showing no cytotoxicity towards L929 cells. The continuously increasing cell viability shows that crosslinked PBISI copolyesters favour the proliferation of L929 cells, suggesting good biocompatibility.

The L929 fibroblast proliferation was also analyzed by SEM to infer the cell adhesion and interaction with substrates. Fig. 12 shows the SEM images of L929 fibroblasts cultured for 3 days on the surface of crosslinked PBISI copolyesters. The images show that the L929 cells adhere well on the surface of crosslinked PBISI copolyesters. The L929 cells grown on the sample are well-expanded in spindle morphologies and form intercellular tight junctions with adjacent cells. There is no significant difference in cell morphology for crosslinked PBISI copolyesters with different ISB content, an indication that crosslinked PBISIs support the adhesion and proliferation of L929 cells very well. The viability and SEM results show that crosslinked PBISIs are potentially biocompatible.

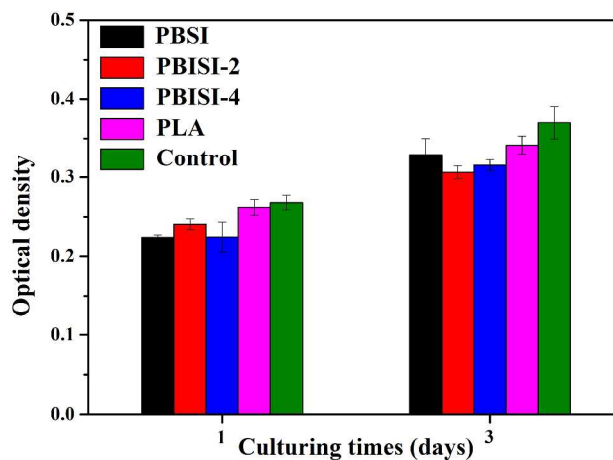


Fig. 11 Optical density of L929 cells cultured on crosslinked PBISI copolyesters. The samples were cured with 0.4 phr of DCP.

4. Conclusions

Biobased PBISI copolyesters with noncytotoxicity were successfully synthesized by polymerizing several commercial biobased monomers, containing isosorbide (ISB), butanediol, itaconic acid and sebacic acid. The composition, melting temperature and crystallinity of the PBISI copolyesters can be tuned continuously by changing the content of ISB. The PBISI copolyesters were crosslinked to form SMPs with excellent shape recovery and fixity (near 100% and independent of thermomechanical cycles). The switching temperatures of PBISI-based SMPs were tuned by introducing ISB into PBISI copolyesters and varying the curing extent. The switching temperature is typical of that for biomedical applications in the human body. Furthermore, the PBISI copolyesters supported the adhesion and proliferation of L929 cells very well. It is believed that these newly developed PBISI-based SMPs are promising candidates for various biomedical applications.

Acknowledgements

This work was supported by the National Natural Science Foundation of China (Grant No. 50933001 and 51221002).

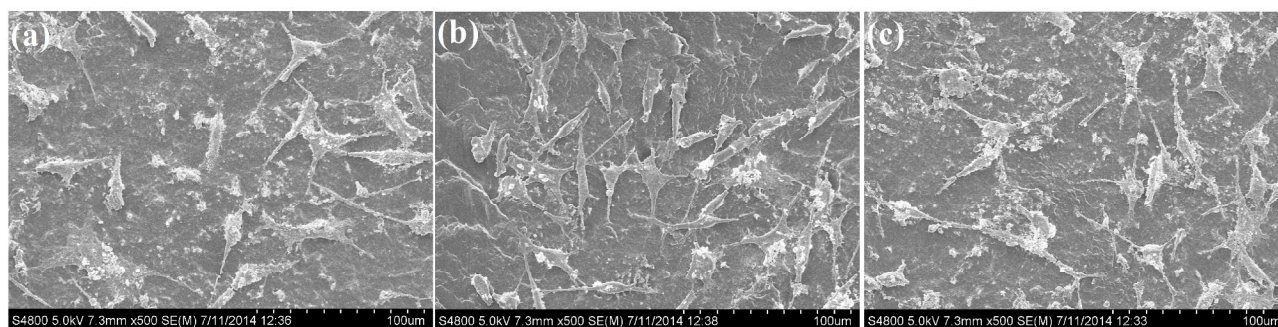


Fig. 12 SEM micrographs showing morphology of L929 cells after 3 days of cell culture on crosslinked (a) PBISI copolyester, (b) PBISI-2 copolyester and (c) PBISI-4 copolyester. The samples were cured with 0.4 phr of DCP.

Notes and references

^aState Key Laboratory of Organic-Inorganic Composites, Beijing University of Chemical Technology, Beijing 100029, P. R. China

^bBeijing Laboratory of Biomedical Materials, Beijing University of Chemical Technology, Beijing 100029, P. R. China

^cDepartment of Polymer Materials and Engineering, South China University of Technology, Guangzhou 510640, P. R. China

^dCollege of Materials Science and Engineering, Shenyang University of Chemical Technology, Shenyang, 110142, China

*Corresponding authors.

Correspondences should be addressed to Prof L. Q. Zhang at ZhangLQ@mail.buct.edu.cn or Prof B. C. Guo at Psbcguo@scut.edu.cn.

[1] A. Lendlein, and S. Kelch, *Angew. Chem. Int. Edit.*, 2002, **41**, 2034-2057.

[2] A. Lendlein, H. Jiang, O. Jünger and R. Langer, *Nature*, 2005, **434**, 879-882.

[3] Z. Tang, D. Sun, D. Yang, B. Guo, L. Zhang and D. Jia, *Compos. Sci. Technol.*, 2013, **75**, 15-21.

[4] A.M. Schmidt, *Macromol. Rapid. Comm.*, 2006, **27**, 1168-1172.

[5] W. Huang, B. Yang, L. An, C. Li and Y. Chan, *Appl. Phys. Lett.*, 2005, **86**, 114105.

[6] A. Alteheld, Y. Feng, S. Kelch and A. Lendlein, *Angew. Chem. Int. Edit.*, 2005, **44**, 1188-1192.

[7] Y. Zhu, J. Hu and K. Yeung, *Acta Biomater.*, 2009, **5**, 3346-3357.

[8] I.S. Kolesov, K. Kratz, A. Lendlein and H.-J. Radusch, *Polymer*, 2009, **50**, 5490-5498.

[9] L. Xue, S. Dai and Z. Li, *Macromolecules*, 2009, **42**, 964-972.

[10] L. Xue, S. Dai, Z. Li, *Biomaterials*, 2010, **31**, 8132-8140.

[11] T. Potta, C. Chun and S.-C. Song, *Biomaterials*, 2010, **31**, 8107-8120.

[12] K. Nagahama, Y. Ueda, T. Ouchi and Y. Ohya, *Biomacromolecules*, 2009, **10**, 1789-1794.

[13] B. Guo, Y. Chen, Y. Lei, L. Zhang, W.Y. Zhou, A.B.M. Rabie and J. Zhao, *Biomacromolecules*, 2011, **12**, 1312-1321.

[14] T. Wei, L. Lei, H. Kang, B. Qiao, Z. Wang, L. Zhang, P. Coates, K.C. Hua, J. Kulig, *Adv. Eng. Mater.*, 2012, **14**, 112-118.

[15] H. Kang, X. Li, J. Xue, L. Zhang, L. Liu, R. Xu and B. Guo, *RSC Adv.*, 2014, **4**, 19462-19471.

[16] D. Garlotta, *J. Polym. Environ.*, 2001, **9**, 63-84.

[17] C. Reddy, R. Ghai and V.C. Kalia, *Bioresource technol.*, 2003, **87**, 137-146.

[18] S. Swain, S. Biswal, P. Nanda and P.L. Nayak, *J. Polym. Environ.*, 2004, **12**, 35-42.

[19] J. Wu, P. Eduard, S. Thiyagarajan, L. Jasinska-Walc, A. Rozanski, C.I.F. Guerra, B.A. Noorderover, J. van Haveren, D.S. van Es and C.E. Koning, *Macromolecules*, 2012, **45**, 5069-5080.

[20] F. Fenouillot, A. Rousseau, G. Colomines, R. Saint-Loup, J.-P. Pascault, *Prog. Polym. Sci.*, 2010, **35**, 578-622.

[21] Z. Wang, X. Zhang, R. Wang, H. Kang, B. Qiao, J. Ma, L. Zhang and H. Wang, *Macromolecules*, 2012, **45**, 9010-9019.

[22] R. Wang, J. Ma, X. Zhou, Z. Wang, H. Kang, L. Zhang, K.-c. Hua and J. Kulig, *Macromolecules*, 2012, **45**, 6830-6839.

[23] A. Gandini, D. Coelho, M. Gomes, B. Reis and A. Silvestre, *J. Mater. Chem.*, 2009, **19**, 8656-8664.

[24] R. Sablong, R. Duchateau, C.E. Koning, G.d. Wit, D.v. Es, R. Koelewijn and J.v. Haveren, *Biomacromolecules*, 2008, **9**, 3090-3097.

[25] B.A. Noorderover, V.G. van Staalduinen, R. Duchateau, C.E. Koning, R.A. van Benthem, M. Mak, A. Heise, A.E. Frissen and J. van Haveren, *Biomacromolecules*, 2006, **7**, 3406-3416.

[26] B.A. Noorderover, R. Duchateau, R.A. van Benthem, W. Ming and C.E. Koning, *Biomacromolecules*, 2007, **8**, 3860-3870.

[27] M. Beldi, R. Medimagh, S. Chatti, S. Marque, D. Prim, A. Loupy and F. Delolme, *Eur. Polym. J.*, 2007, **43**, 3415-3433.

[28] L. Jasinska, M. Villani, J. Wu, D. van Es, E. Klop, S. Rastogi and C.E. Koning, *Macromolecules*, 2011, **44**, 3458-3466.

[29] S. Chatti, G. Schwarz and H.R. Kricheldorf, *Macromolecules*, 2006, **39**, 9064-9070.

[30] R. Storbeck and M. Ballauff, *J. Appl. Polym. Sci.*, 1996, **59**, 1199-1202.

[31] H. Kricheldorf, G. Behnken and M. Sell, *J. Macromol. Sci. Pure*, 2007, **44**, 679-684.

[32] C. Japu, A. Alla, A.M. de Ilarduya, M.G. García-Martín, E. Benito, J.A. Galbis and S. Muñoz-Guerra, *Polym. Chem.*, 2012, **3**, 2092-2101.

[33] C. Japu, A. Martínez de Ilarduya, A. Alla, M.G. Garcia-Martin, J.A. Galbis and S. Muñoz-Guerra, *Polym. Chem.*, 2013, **4**, 3524-3536.

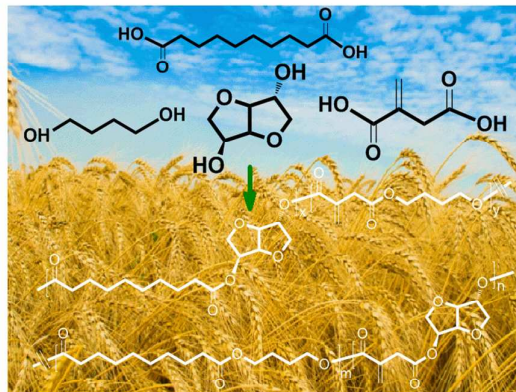
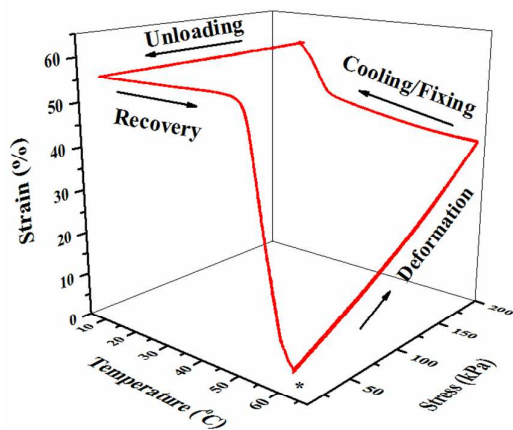
[34] C. Liu, S.B. Chun, P.T. Mather, L. Zheng, E.H. Haley and E.B. Coughlin, *Macromolecules*, 2002, **35**, 9868-9874.

[35] M. Behl, M.Y. Razzaq and A. Lendlein, *Adv. Mater.*, 2010, **22**, 3388-3410.

[36] H.M.D. Millesi, G.M.D. Zoch and R.P. Reihnsner, *Clin. Orthop.*, 1995.

[37] H.W. Sung, Y. Chang, C.T. Chiu, C.N. Chen and H.C. Liang, *Biomaterials*, 1999, **20**, 1759-1772.

Graphical Abstract:



Isosorbide-based SMPs